



Preparation of biopolymer/CuO-magadiite biocomposite beads by chemical reduction method and their antibacterial activity

Adel Mokhtar^{1, 2*}, Soumia Abdelkrim¹, Amal Djelad¹, Abdelkader Bengueddach¹ & Mohamed Sassi¹

¹Laboratoire de Chimie des Matériaux, Département de Chimie, Faculté des Sciences exactes et Appliquées. Université Oran1. B.P 1524 El-Menaouer, 31000 Oran, Algeria.

²Département de sciences techniques, Centre universitaire Ahmed Zabana de Relizane, Route de l'hôpital, 48000 Relizane, Algeria

Article history: Received 31 May 2019. Accepted 25 July 2019

Abstract. In this work, an inorganic-organic nanocomposite material was prepared by combining copper exchanged-magadiite (Cu-magadiite) material with chitosan. The synthesis was carried out by direct dispersion of the Cu-magadiite in the chitosan matrix. The mixture obtained is shaped into beads with an average diameter of about 1~1.2 mm. These beads were then contacted with a solution of NaBH₄ in ethanol in order to reduce loaded copper ions into copper nanoparticles species. The resulting nanocomposite material, named Cu-NPs-magadiite/chitosan, was characterized by X-ray diffraction (XRD), Fourier transforms infrared spectroscopy (FTIR), scanning electron microscopy (SEM), Thermogravimetric (TG), UV-Visible diffuse reflectance (UV-Visible DR) and EDX analysis. The results show that the layered silicate magadiite was completely exfoliated confirming the formation of the organic-inorganic composite material. Indeed, the encapsulation of the layered silicate was confirmed by the SEM images, which is presented as micron free aggregates included in the cavities of a continuous polysaccharide matrix. Otherwise, they confirm also the formation of copper nanoparticles (CuNPs) which are probably immobilized inside the magadiite-chitosan solid matrix. The antibacterial activity against *Escherichia coli* and *Staphylococcus aureus* of the nanocomposite was highlighted by the disc inhibition method and the minimum inhibitory concentration (MIC) was determined. The CuNPs-magadiite/chitosan nanocomposite material showed a very efficient bactericidal effect against both pathogen *E. Coli* and *staphylococcus* bacteria strains. Additionally, the MIC values obtained for nanocomposite are of 0.25 µg/L against *S. aureus* and of 0.50 µg/L against *E. coli*. Therefore, encapsulation of low levels of magadiite as a carrier for copper ions in the chitosan matrix has proven to be a good method for developing functional composites that can potentially be applied as antibacterial agents against pathogen gram+ and gram- bacterial strains.

Keywords: Chitosan-magadiite-nanocomposite beads-NaBH₄-antibacterial activity.

1 Introduction

Metallic ions such as Ag⁺, Cu²⁺, Ni²⁺, Ce³⁺ and Zn²⁺ and their metal oxide (CuO, ZnO and TiO₂) and nanoparticles species were recently widely applied against different pathogen bacteria due to their intrinsic antibacterial activities. Driven by human health and environmental concern and economic consideration, these antibacterial metals were not used alone. Thus, several metal nanoparticles and metal-containing materials and coating with antimicrobial activity, especially

* Corresponding author. Adel Mokhtar .
E-mail address: mokhtar.adel80@yahoo.com

silver and copper, were developed and used in several fields such as in medicine against several resistant bacteria strains, in wastewater treatment, in textile. However, the direct inclusion of these agents in composite material formulations was limited by uncontrolled leaching which may adversely affect human health. Unless, to limit or ovoid this phenomenon, many process were used to immobilize these different metal species into inorganic and/or organic carriers, i.e., zeolites, clay minerals, polymers and layered silicate, especially since recent works have shown that the antimicrobial activity of these metal nanoparticles is due to their small size and their very high surface area compared to their small volume which allows them to interact directly with the microbial membrane without however being released in solution.

Magadiite is a natural crystalline hydrated sodium silicate discovered by Eugster in lake Magadii. This solid mineral can be easily prepared in the laboratory under hydrothermal conditions[1]. It's interesting properties such as easily exchangeable interlayer Na^+ cations, water molecules and reactive silanol groups are at the origin of the development of several composite materials for different applications such as catalysts [2], antibacterial materials or adsorbents [3, 4]. Biopolymers and layered silicate materials does not show any antibacterial activity alone, in order to impart that activity, it is necessary to incorporate some antibacterial agents such as mentioned above. Magadiite has previously been investigated as antibacterial material by ion-exchange reaction with copper ions [3]. On the other hand, Chitosan has widely investigated as matrix to incorporate antibacterial nanoparticles like ZnO, Ag, CuO or Au nanoparticles. The formation of nanocomposites by combination of a polymer and a lamellar inorganic material generates various properties which depend of synthesis method and to the state of provided nanocomposite, the conventional composite, intercalated nanocomposite, or exfoliated nanocomposite. This produces and enhances various properties such as thermal stability, biodegradability, mechanical and electrical properties. These properties have been the conclusion of many attractions for many applications such as antibacterial activity [5, 6], dye and heavy metal removal [7, 8], food packaging [9] and fireproof [10], ect.

Due to the polycationic nature of chitosan in acidic media [14, 15], this biopolymer can be formed a composite materials beads with Na-magadiite by cationic exchanges and hydrogen bonding methods, the resulting nanocomposites having interesting structural and functional properties. Until now, there is no paper reporting on the design of a nanocomposite based on copper-magadiite nanoparticles encapsulated chitosan matrix. In this study, Cu-Magadiite was prepared by ion exchange in aqueous solution first and then mixed with the acidified aqueous solution of chitosan. After that the NaBH_4 and NaOH solution was used to reduce the copper ions. The prepared materials were subjected to different characterization and their antibacterial activity was evaluated.

2. Materials and methods

2.1. Materials

Chitosan (degree of acetylation of 10% as measured by IR spectroscopy, $\text{MW} = 700\,000 \text{ g.mol}^{-1}$ determined by viscosimetry) from crab shell, sodium tripolyphosphate (STPP, technical grade 85%), Sodium borohydride (NaBH_4) 90% , silica Ludox AS-40 and copper nitrate hexahydrate

were obtained from Sigma-Aldrich, the sodium hydroxide from Fluka and deionized water were used for all preparations.

2.2. Preparation of Na-magadiite, Cu-magadiite and chitosan/CuNPs-magadiite nanocomposite

2.2.1. Na-magadiite

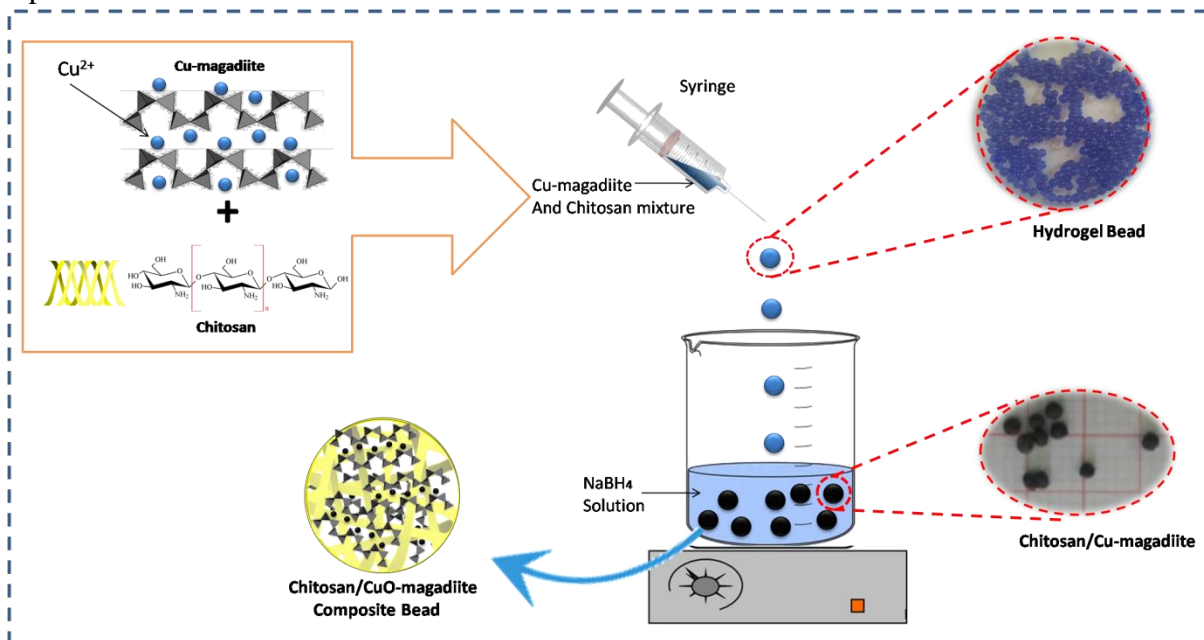
Na-magadiite was synthesized following the procedure described in the literature [1, 11, 12]. A molar composition $\text{SiO}_2/\text{NaOH}/\text{H}_2\text{O} = 9:3:162$, was mixed and stirred for three hours at room temperature. The gel obtained was transferred into a Teflon-lined stainless steel autoclave and maintained at 150°C during 48 hours under autogenous pressure. The solid obtained was washed several time with desionized water to remove excess of NaOH until $\text{pH} = 9.0\sim 11$ and then dried in air at 70°C during 48 hours.

2.2.2. Cu-magadiite

The preparation of Cu-magadiite material, described in a previous work [13], was carried out by ion-exchange method as follows: 1.5g of the as-synthesized Na-magadiite was suspended in deionized water and stirred for 30 minutes. Then, a copper solution prepared by dissolving the required amount of $\text{Cu}(\text{NO}_3)_2$ in desionized water was added. The reaction mixture obtained was vigorously stirred for 48 hours at 30°C . To avoid undesirable proton exchange reaction, solutions were stabilized at $\text{pH} 5.6$. The resulting Cu-magadiite samples were recovered by filtration, and then dried at 70°C for 24 hours.

2.2.3. CuNPs-magadiite/chitosan nanocomposite

The CuNPs-magadiite/chitosan nanocomposite (see scheme 1) were prepared according to a previously reported technique method with some modification [14]. 0.5g of Cu-magadiite sample prepared as before was first added to 12.5ml of deionized water and stirred for 1 hour at 30°C .



Scheme. 1. Preparation method of CuNPs-magadiite/chitosan nanocomposite.

This dispersion is named solution 1. A solution 2 was prepared by dissolving chitosan under stirring for 45 minutes at 45°C in 1 wt.% acetic acid solution to obtain 1 wt.% chitosan solution. This solution chitosan was filtered to remove the insoluble chitosan. Then, Both solution 1 and solution 2 were mixed vigorously under stirred conditions. After three hour of reaction, the mixture solution was extruded in the form of droplets, using a syringe (2 mm diameter), into an ethanol solution containing sodium borohydride (NaBH₄). The formed beads were stayed in the solution for two h in order to crosslink with NaBH₄ and also converting Cu ions into CuNPs. After that, the beads were filtered and washed several times with distilled water to remove unreacted NaBH₄ and NaOH and dried under vacuum for 24h.

2.3. Characterization technique

X-ray powder diffraction (XRD) patterns were recorded in the 2θ range of 2-70° at a scan rate 2°/min, on a Philips diffractometer model PW 1830, with Ni-filtered CuKα (λ= 1.5406 Å) radiation operated at a tube voltage of 40 kV and a tube current of 30 mA. The Fourier Transform infrared (FTIR) spectra were recorded between 400 and 4000 cm⁻¹ on a JASCO 4100 spectrometer. Ultraviolet visible diffuse reflectance (UV-Vis DR) spectroscopy were recorded on a Specord 210 Analytik Jena spectrometer with a holmium oxide filter. The morphological features of samples were investigated using a PHILIPS XL30 scanning electron microscope.

2.4. Antibacterial activity

Antibacterial activity of the CuNPs-magadiite/chitosan nanocomposite was tested against bacteria under references: Escherichia coli (ATCC 25922) and Staphylococcus aureus (ATCC 29213). The culture medium was prepared by Mueller-Hinton agar (MH) is a rich agar for the realization of the standard antibiogram, it allows diffusion of inhibition product appropriately with the addition of agar and water Distilled 9 ml per tube for bacterial dilution and suspension in liquid medium. The method used is EYMARD 2003. The method consists of culturing young bacteria in culture medium (MH), a volume of 10-1-10-3 ml of culture (10⁵ cells/ml) obtained after incubation at 37°C. For 18 h is mixed with the medium (MH), a circular hole is cut in the agar about 6 mm, the discs of the materials to be tested are then deposited in the holes our products, four materials per box (3 cm Each product). The petri dishes, containing the mixtures, are then incubated at 37 °C. Until zones of bacterial inhibition appear. The inhibition appears as a clear halo around the discs. After twenty-four hours of contact at 37°C. of the bacterial solid-solid, the petri dishes are removed from the incubator and immediately photographed, after that the inhibition zone for bacterial growth was detected visually.

3. Results and discussions

3.1. X-ray diffraction (XRD) analysis

The powder XRD patterns of Na-magadiite, Cu-magadiite and CuNPs-magadiite/chitosan nanocomposite are shown in **Fig. 1**. The powder XRD pattern of Na-magadiite displayed all the reflections (00*l*) corresponding to the basal spacing, d₀₀₁, of 1.56nm characteristic of such a material, in good agreement with previous works [15, 16]. The powder XRD pattern of Cu-

magadiite sample shows a decrease in the basal spacing from 1.56nm to 1.36nm. This behavior is probably due to the exchange of large hydrated sodium ions by unhydrated small copper ions, confirming the intercalation of copper ions between the silicate layers. As well as there is appearance of the new diffraction peaks assigned to the corresponding copper hydroxide phases [17]. The XRD powder of CuNPs-magadiite/chitosan nanocomposite beads shows a disappearance of characteristic the (001) basal reflection peak implying that the layered silicate magadiite could be in exfoliated state [18-22]. This important result reveal that the interlayer spacing of magadiite was swollen by chitosan biopolymer molecules leading to predominantly exfoliation of this material as well as to the formation of strong interactions chitosan-silicate layers which could influence the crystalline properties of layered silicate magadiite structure [23].

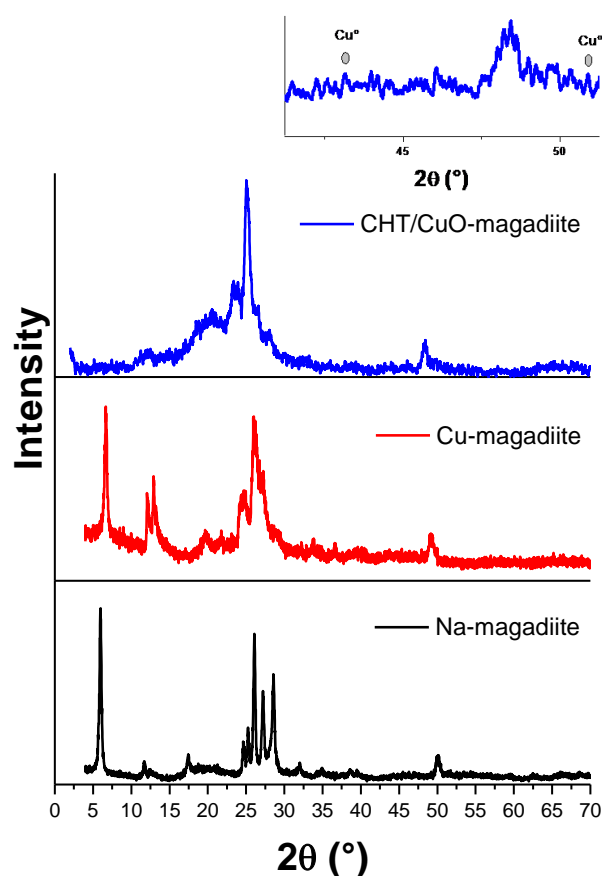


Fig. 1 Powder XRD patterns of Na-magadiite, Cu-magadiite and CuNPs-magadiite/chitosan nanocomposite materials.

Despite the large amount of chitosan used (1/3) compared to the amount of Cu-magadiite, the characteristic peaks of the silicate layer of magadiite are detected in the nanocomposite. According to the literature [24, 25], the large reflection line observed between 20° and 25° is attributed to chitosan. The powder XRD pattern of CuNPs-magadiite/chitosan shows the relative intensities of the Cu° diffraction peaks suggesting that the reduction has been well done and the formation of the copper nanoparticles species [14, 26, 27]. Peaks detected at 2θ values of 43.39° and 50.49° correspond to (111) and (200) planes of metallic Cu reflections (JCPDS file no. 05-0667) [28]. An oxidation reaction is produced due to presence of copper hydroxide phase in Cu-

magadiite this allows the formation of a mixture of copper oxide CuO, Cu₂O in CuNPs-magadiite/chitosan nanocomposite [29, 30]. Indeed, the peaks are not clear with low intensity which can be explained by the small amount of copper ions used in exchanged process with magadiite and the large dispersion of copper into the layer silicate magadiite.

3.2. UV–Visible diffuse reflectance (UV-Vis DR) spectroscopy analysis

The UV–Vis DR spectra were recorded in order to have more information about the coordination and the oxidation states of copper in Cu-magadiite and CuNPs-magadiite/chitosan samples. The UV–Vis DR spectra of the Na-magadiite, Cu-magadiite and CuNPs-magadiite/chitosan nanocomposite beads are displayed in the **Fig. 2**. The Na-magadiite material displays a large absorption band between 200nm and 300nm with a shoulder at about 250nm attributed to silica wavelength region [31, 32].

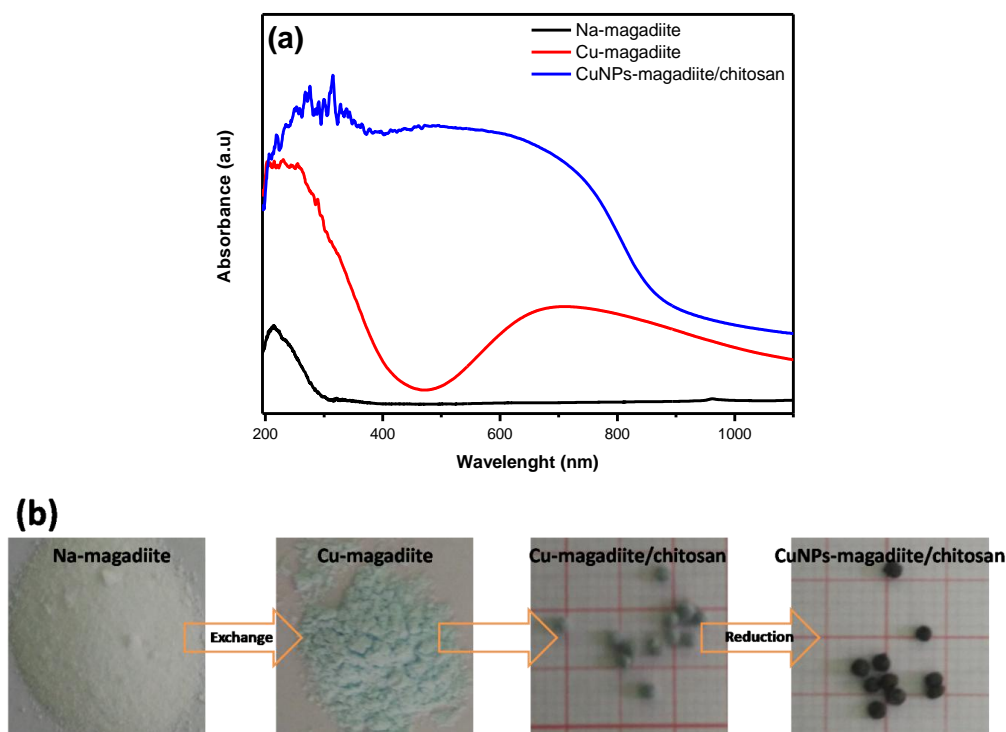


Fig. 2 UV–Vis DR spectra (a) of Na-magadiite, Cu-magadiite and CuNPs-magadiite/chitosan nanocomposite.

The Cu-magadiite material shows two absorption bands in UV–Vis DR spectral region between 200-1000 nm. The first band observed between 220-260 nm can be attributed to a charge transfer (CT) O→Cu transitions of isolated Cu²⁺ ions in coordination with lattice oxygen. The second band broader and less intense observed between 680-800 nm is attributed to *d-d* transition of Cu²⁺ [33-35].

After NaBH₄ reduction, the color of the resulting CuNPs-magadiite/chitosan nanocomposite changed from blue to bronze (see figure), indicating probably the formation of CuNPs species. The UV–Vis DR spectra of nanocomposite shows the appearance of a new absorption peak centered between 500 and 600 nm that can be attributed to the presence of copper nanoparticles species. The adsorption peak is very broad and present an asymmetric peak shape which suggests

that the formed CuNPs nanoparticles have different size distribution. On the basis on these data, it appears that the use of NaBH_4 leads to the reduction of a part of Cu^{2+} ions into Cu^0 species, confirming the presence in the CuNPs-magadiite/chitosan nanocomposite of different copper species. The latter are in form of CuNPs with different size distribution.

the color of the prepared material changes from white (no Cu) to light blue (presence of copper ions), to black (presence of CuNPs).

3.3. Fourier transform infrared (FTIR) spectroscopy analysis

The FTIR spectra of Na-magadiite, Cu-magadiite and CuNPs-magadiite/chitosan nanocomposite are shown in **Fig. 3**. The FTIR spectrum of Na-magadiite displays all the vibration bands characteristics of this layered silicate in accordance with the literature [13, 32, 36, 37]. Its divided in two parts, the first one between 3000 cm^{-1} and 4000 cm^{-1} is attributed to the vibration of interlayer water molecules and second one between 400 cm^{-1} and 1600 cm^{-1} corresponds to the vibration of the silicate layer. Thus, the medium band at 1230 cm^{-1} is assigned to the vibration of the five membered ring groups characteristic of this material. The very strong band at 1100 cm^{-1} with a shoulder at 1130 cm^{-1} is assigned to the vibration of interlayer Si-O^- groups. The bands observed between 700 cm^{-1} and 470 cm^{-1} are assigned to the symmetric stretching vibration of the Si-O-Si groups. The narrow absorption band at 3662 cm^{-1} is due to the presence of isolated silanol groups, Si-OH . The very broad absorption band centered at 3435 cm^{-1} is assigned to the vibrations of OH groups involved in strong interlayer hydrogen bands, $\text{Si-OH}\cdots\text{O}$, as well as to the interlayer water molecules. Finally, the absorption band observed at 1620 cm^{-1} is due to the binding vibration of physisorbed water molecules. After exchange reaction with copper ions, the FTIR spectrum of Cu-magadiite shows no more absorption bands indicating that ion exchange reaction did not markedly affect the magadiite framework.

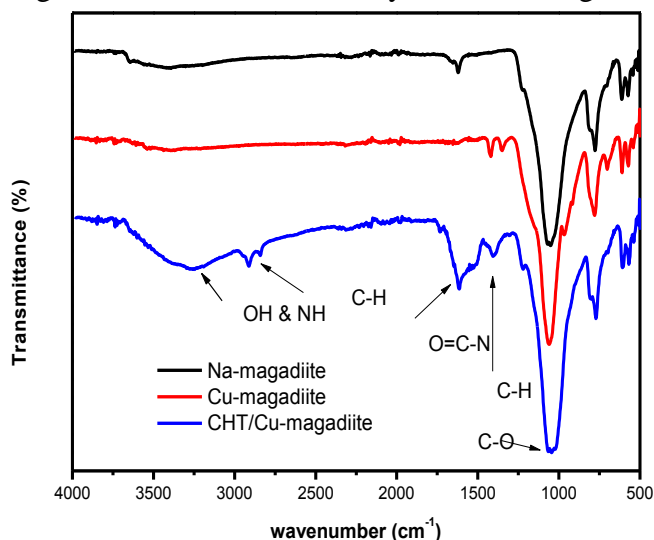


Fig. 3 FTIR spectra of Na-magadiite, Cu-magadiite and CuNPs-magadiite/chitosan nanocomposite materials

In addition to the absorption bands of magadiite, the FTIR spectrum of CuNPs-magadiite/chitosan nanocomposite material presented also the absorption bands characteristic of chitosan. The absorption bands observed at 2923 cm^{-1} and 2874 cm^{-1} are attributed to the stretching vibration of $-\text{CH}$ in $-\text{CH}_2$ and $-\text{CH}_3$ groups, respectively. The bending vibrations of

the same bond appeared at 1422 and 1379 cm^{-1} . The absorption bands of $-\text{C}-\text{O}-\text{C}-$ in the glycosidic linkages and $\text{C}-\text{O}$ bond in the amide group were observed at 1159 and 1089 cm^{-1} , respectively. The intensity of these bands weakened, due might be owed to the overlapping of $\text{Si}-\text{O}-\text{Si}$ absorbance band [38]. In summary, FTIR results reveal that chitosan hydroxyl groups as well as amine groups may bond with $\text{Si}-\text{O}-\text{Si}$ groups of the silicate layer of magadiite.

3.4. Scanning electron microscopy analysis

Figure 5 shows the SEM images of the synthesis Na-magadiite and CuNPs-magadiite/chitosan nanocomposite. The as-synthesised Na-magadiite sample possessed the typical cauliflower morphology with open aggregation of plates of around $\sim 12\text{--}15\ \mu\text{m}$ characteristic of such a material [1], [39].

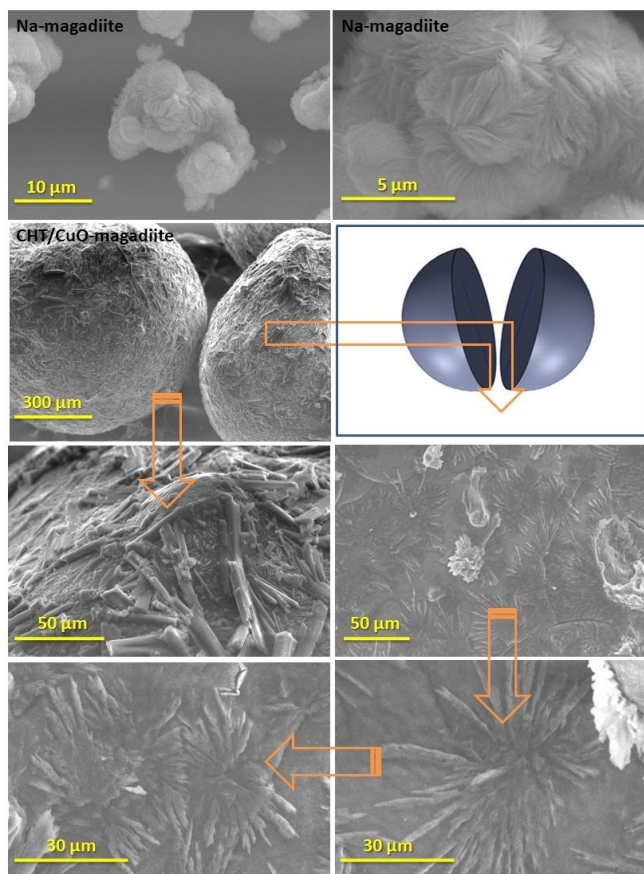


Fig. 4 SEM micrographs of Na-magadiite and CuNPs-magadiite/chitosan nanocomposite.

The product is highly crystalline and pure. The SEM micrograph of the CuNPs-magadiite/Chitosan nanocomposite material shows that magadiite is encapsulated by chitosan. The layered silicate magadiite is present as micrometer free aggregates included in the cavities of a continuous polysaccharide matrix, indicating that the layered structure is exfoliated in good agreement with the XRD results. In addition, the evaporation drying steps gives that removal of the polysaccharide gel has resulted in a physical coating between polymer and incorporated magadiite layers.

The typical EDX spectrum of CuNPs-magadiite/chitosan nanocomposite is shown in **Fig. 5**. The spectrum indicated the existence of C, O, N, Na, Si and Cu elements. The peaks situated at

binding energies of 0.85, 0.94, 8.04 and 8.94 keV correspond to CuL_1 , CuL_α , CuK_α and CuK_β [28], respectively. These are similar to that reported in previous works and indicate the presence of different copper nanoparticles species which are most likely in the form of copper nanoparticles (CuNPs). However, according to the DRUV results, the formation also of copper oxide species such as CuO and Cu_2O cannot be ruled up [40].

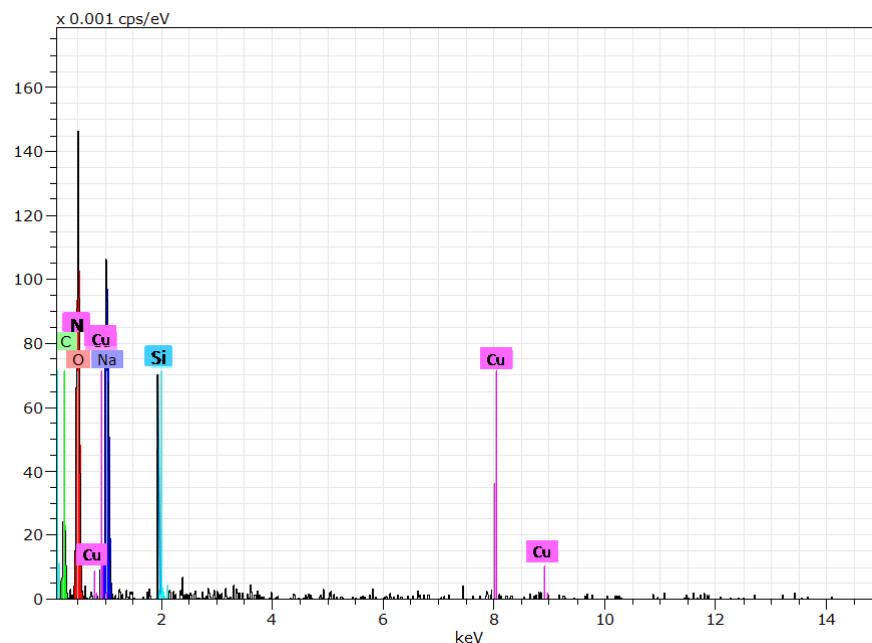


Fig. 5. EDX spectrum of CuNPs-magadiite/chitosan nanocomposite.

Thermogravimetric (TG)

The thermal stability of the chitosan and CuNPs-magadiite/chitosan nanocomposite has been investigated by TG under air flows (**Fig. 6**), the TG curve of Na-magadiite was also showed inside. There are three steps of weight loss. The first range (50-200 °C) is associated with the loss of water about 6-9 wt%, whereas the second range (200-450 °C) corresponds to the degradation and deacetylation of chitosan and left about ~52 wt% solid residue. This is comparable to the results reported by other researchers [41]. In the last weight loss at region of (450-700 °C) is another degradation, which may be assigned to the oxidative degradation of the carbonaceous residue formed during the second step. In the case of CuNPs-magadiite/chitosan nanocomposite, the TG curve shows three stages of mass loss as in the case of chitosan. The difference has been in the loss of water which is lower than that of chitosan due to evaporation process. In fact, the temperature of the loss of mass attributed to the dehydroxylation of magadiite layers and the degradation and combustion of chitosan increases over pure chitosan and Na-magadiite. The observed thermal stabilization is probably due to the barrier provided by the platelets to the diffusion of oxygen and the encapsulation of the layer silicate which causes a restricted thermal movement and probably also due to the presence of nanoparticles which improves the thermal stability of the nanocomposite material. It can be seen that the thermal stability of chitosan in the nanocomposite material has increased after encapsulation process.

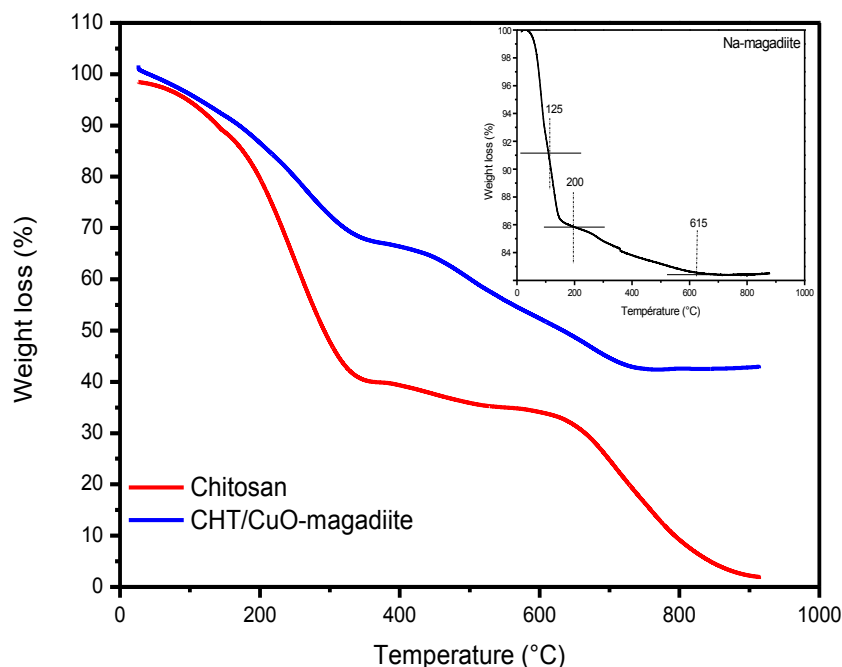


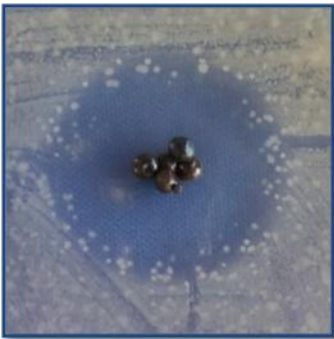
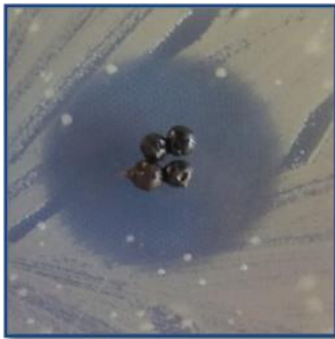
Figure. 6 Thermogravimetric analysis curves for Chitosan, CuNPs-magadiite/chitosan nanocomposite and Na-magadiite (inside figure).

3.4. Antibacterial properties

In order to investigate the antibacterial properties of CuNPs-magadiite/chitosan nanocomposite, the prepared material were tested by disk diffusion test and minimum inhibitory concentration (MIC) techniques against *Escherichia coli* (ATCC 25922) Gram-negative and *Staphylococcus aureus* (ATCC 29213) Gram-negative. These pathogenic bacteria were selected because they are commonly known to cause human infections⁴². The diameter of the inhibition zone in the disk is given in millimeters. The tests were repeated three times, and the results are presented in Table 1. CuNPs-magadiite/chitosan nanocomposite shows a more interesting antibacterial activity, the inhibition zone was very clear with a larger diameter, which gives zone diameters of 24 mm and 25 mm for bacterial media containing *Escherichia coli* and *Staphylococcus aureus*, respectively. The activity probably depends on the presence of copper loaded in the layer silicate magadiite as well as by the reduction of copper. The antibacterial activity results demonstrated that the exhibit a very good antibacterial activity and the morphology of the nanocomposite can acting an important role. The antibacterial activity was attributed to the property of the copper ions and, especially when reduced to CuNPs the activity was better.


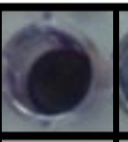






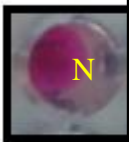

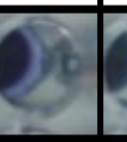



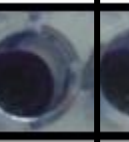

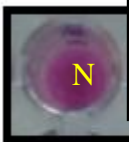
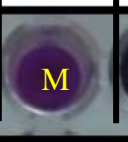

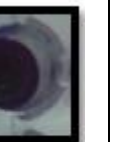

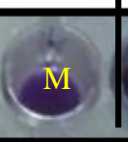
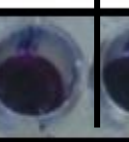

Various mechanisms have been suggested for the antibacterial activity of nanoparticles, including generation of oxygen species to degradation of cell structure or release of ions from the surface of nanoparticles to binding the cell membrane. The beads CuNPs-magadiite/chitosan nanocomposite probably attracted the bacteria by electrostatic forces, then immobilized them on the surface, and at the same time, the CuNPs released and exerted its antibacterial effect directly on the bacteria.

Table 1 Antimicrobial activity against *Escherichia coli* and *Staphylococcus aureus* measured as inhibition zone expressed as millimeter (mm) of CHT/CuNPs-magadiite.

Bacteria	<i>Escherichia coli</i> Gram-negative	<i>Staphylococcus aureus</i> Gram-positive
CuNPs-magadiite/chitosan nanocomposite		
	24.0 ± 0.5	25.0 ± 0.5

The Minimum inhibitory concentration (MIC) was determined using the method of Sarker et al (2007) as shown in Table 2. This technique consists of dosing on micro-plates, the products have been tested in triplicate and the microplate which contain 200µg of Ciprolon (Ciprofloxacin) antibiotic was used as a positive control, and DMSO was used as a negative control. The (MIC) of was determined by the weakest concentration agent that completely inhibits visible growth, as judged by the naked eye against bacteria (*Escherichia coli* and *Staphylococcus aureus*).

Table 2 Microtiter ELISA plate and CIM of (A) antibiotic Ciprofloxacin, (B) CuNPs-magadiite/chitosan nanocomposite and (C) Cu-magadiite/chitosan not reduced.

Bacteria	<i>Escherichia coli</i> (ATCC 25922) Gram-negative				<i>Staphylococcus aureus</i> (ATCC 29213). Gram-positive			
	0.25	0.50	0.75	1	0.25	0.50	0.75	1
A								
B								
C								

H: High activity, *M*: Moderate and *N*: Non

MIC values have been varied from 0.25 to 1 µg/ml. The MIC values obtained for CuNPs-magadiite/chitosan nanocomposite of 0.25µg/ml against *Staphylococcus aureus* and of 0.50 µg/L against *Escherichia coli*. In the case of Cu-magadiite/chitosan (without reduction method) the

CMI values were more than CuNPs-magadiite/chitosan nanocomposite, for both bacteria the value was 0.75µg/L.

These results indicate that Cu-magadiite/chitosan and CuNPs-magadiite/chitosan nanocomposite showed antibacterial activity against both Gram-positive and Gram-negative bacteria because of the loading of copper, but when the copper ions were reduced the antibacterial effect is better.

4. Conclusion

CuNPs were successfully prepared from Cu-magadiite/chitosan composite beads using NaBH₄ as a chemical reduction agent in the interlamellar space of layered silicate magadiite encapsulated with chitosan without any heat treatment. In conclusion, this work shows the in situ preparation of CuNPs and the antibacterial activity of the beads CuNPs-magadiite/chitosan nanocomposite. The X-ray diffraction suggested that the exfoliation is the majority than the intercalation for layer silicate magadiite and indicated that the chitosan molecular could influence the crystalline properties of layer silicate magadiite structure, and Fourier Transform spectroscopy given the presence of all characteristics bands for both materials chitosan and magadiite. Were confirming the formation of CuNPs-magadiite/chitosan nanocomposite. Moreover, UV-Visible diffuse reflectance shows the information corresponding to the coordination and different oxidation states of metal Cu ions presented in the Cu-magadiite and CuNPs-magadiite/chitosan nanocomposite, the adsorption band observed between region 420-460 nm attributed to CuO species. This result can also confirmed by change in the color of beads from bleu to black. Antibacterial activity of the Cu-magadiite, CHT/Cu-magadiite and CHT/CuNPs-magadiite was examined for against bacteria under references: Escherichia coli (ATCC 25922) and Staphylococcus aureus (ATCC 29213). The results shown that the antibacterial resistance could be modified as a function of the distribution and reduction of the ions possessing the antibacterial activity, and its can also be dependent of the morphology of materials in beads form. The antibacterial activities of CuNPs-magadiite/chitosan nanocomposite showed strong antibacterial activity against Gram-positive and Gram-negative bacteria. Further studies are required to investigate the bactericidal effects of CuNPs-magadiite/chitosan nanocomposite against different types of bacteria for potential widening of their applications.

References

1. Y.-R. Wang, S.-F. Wang and L.-C. Chang, Applied Clay Science **33** (1), 73-77 (2006).
2. G. L. Paz, E. C. Munsignatti and H. O. Pastore, Journal of Molecular Catalysis A: Chemical **422**, 43-50 (2016).
3. A. Mokhtar, A. Djelad, A. Boudia, M. Sassi and A. Bengueddach, Journal of Porous Materials, 1-10 (2017).
4. S. Benkhatou, A. Djelad, M. Sassi, M. Boucekara and A. Bengueddach, Desalination and Water Treatment **57** (20), 9383-9395 (2016).
5. M. Lavorgna, I. Attianese, G. Buonocore, A. Conte, M. Del Nobile, F. Tescione and E. Amendola, Carbohydrate polymers **102**, 385-392 (2014).
6. Y.-S. Han, S.-H. Lee, K. H. Choi and I. Park, Journal of Physics and Chemistry of Solids **71** (4), 464-467 (2010).
7. W. W. Ngah, L. Teong and M. Hanafiah, Carbohydrate polymers **83** (4), 1446-1456 (2011).

8. H. J. Kumari, P. Krishnamoorthy, T. Arumugam, S. Radhakrishnan and D. Vasudevan, International journal of biological macromolecules **96**, 324-333 (2017).
9. J.-W. Rhim, H.-M. Park and C.-S. Ha, Progress in polymer science **38** (10), 1629-1652 (2013).
10. G. Laufer, C. Kirkland, A. A. Cain and J. C. Grunlan, ACS Applied Materials & Interfaces **4** (3), 1643-1649 (2012).
11. R. A. Fletcher and D. M. Bibby, Clays and Clay Minerals **35** (4), 318-320 (1987).
12. F. Feng and K. J. Balkus, Journal of Porous Materials **10** (1), 5-15 (2003).
13. A. Mokhtar, Z. A. K. Medjhoua, A. Djelad, A. Boudia, A. Bengueddach and M. Sassi, Chemical Papers, 1-12.
14. S. Farhoudian, M. Yadollahi and H. Namazi, International journal of biological macromolecules **82**, 837-843 (2016).
15. G. Brindley, American Mineralogist **54** (11-1), 1583-& (1969).
16. W. Schwieger, G. Lagaly, S. Auerbach, K. Carrado and P. Dutta, (Marcel Dekker, Inc., New York, 2004).
17. W. Lim, J.-H. Jang, N.-Y. Park, S.-M. Paek, W.-C. Kim and M. Park, Journal of Materials Chemistry A **5** (8), 4144-4149 (2017).
18. S. Wang, L. Shen, Y. Tong, L. Chen, I. Phang, P. Lim and T. Liu, Polymer Degradation and Stability **90** (1), 123-131 (2005).
19. Z. Wang and T. J. Pinnavaia, Chemistry of Materials **10** (7), 1820-1826 (1998).
20. P. Sun, J. Zhu, T. Chen, Z. Yuan, B. Li, Q. Jin, D. Ding and A. Shi, Chinese Science Bulletin **49** (15), 1664-1666 (2004).
21. N. Bleiman and Y. G. Mishael, Journal of hazardous materials **183** (1), 590-595 (2010).
22. T. Chen, J. Zhu, B. Li, S. Guo, Z. Yuan, P. Sun, D. Ding and A.-C. Shi, Macromolecules **38** (9), 4030-4033 (2005).
23. J. Liu, W.-J. Boo, A. Clearfield and H.-J. Sue, Materials and Manufacturing Processes **21** (2), 143-151 (2006).
24. R. J. Samuels, Journal of Polymer Science Part B: Polymer Physics **19** (7), 1081-1105 (1981).
25. K. Ogawa and T. Yui, Bioscience, biotechnology, and biochemistry **57** (9), 1466-1469 (1993).
26. S. Sohrabnezhad, M. M. Moghaddam and T. Salavatiyan, Spectrochimica Acta Part A: Molecular and Biomolecular Spectroscopy **125**, 73-78 (2014).
27. M. He, M. Luo and P. Fang, Journal of Rare Earths **24** (2), 188-192 (2006).
28. A. Khan, A. Rashid, R. Younas and R. Chong, International Nano Letters **6** (1), 21-26 (2016).
29. M. KOUTI and L. Matouri, (2010).
30. P. Kanninen, C. Johans, J. Merta and K. Kontturi, Journal of colloid and interface science **318** (1), 88-95 (2008).
31. Y. Chen and G. Yu, Clay Minerals **48** (5), 739-748 (2013).
32. Y. Chen, G. Yu, F. Li and J. Wei, Applied clay science **88**, 163-169 (2014).
33. I. R. Iznaga, V. Petranovskii, G. R. Fuentes, C. Mendoza and A. B. Aguilar, Journal of colloid and interface science **316** (2), 877-886 (2007).
34. S. Velu, K. Suzuki, S. Hashimoto, N. Satoh, F. Ohashi and S. Tomura, Journal of Materials Chemistry **11** (8), 2049-2060 (2001).
35. Z. Ismagilov, S. Yashnik, V. Anufrienko, T. Larina, N. Vasenin, N. Bulgakov, S. Vosel and L. Tsykoza, Applied surface science **226** (1), 88-93 (2004).
36. Y. Huang, Z. Jiang and W. Schwieger, Chemistry of Materials **11** (5), 1210-1217 (1999).
37. A. R. Nunes, A. O. Moura and A. G. Prado, Journal of Thermal analysis and Calorimetry **106** (2), 445-452 (2011).
38. C. Paluszkiwicz, E. Stodolak, M. Hasik and M. Blazewicz, Spectrochimica Acta Part A: Molecular and Biomolecular Spectroscopy **79** (4), 784-788 (2011).
39. Q. Wang, Y. Zhang, J. Zheng, Y. Wang, T. Hu and C. Meng, Dalton Transactions (2017).
40. A. K. Sasmal, S. Dutta and T. Pal, Dalton Transactions **45** (7), 3139-3150 (2016).
41. X. Qu, A. Wirsén and A.-C. Albertsson, Polymer **41** (13), 4841-4847 (2000).
42. S. A. M. Hanim, N. A. N. N. Malek and Z. Ibrahim, Applied surface science **360**, 121-130 (2016).